# Effect on Structural, Micro Structural and Optical Properties due to Change in Composition of Zn and Sn in ZnO:SnO₂ Nanocomposite Thin Films

L.A. Patil[1,*], I.G. Pathan[2], D.N. Suryawanshi[3], D.M. Patil[1]

[1] *Nanomaterials Research Lab., Pratap College, Amalner 425 001, India*
[2] *Arts, Commerce and Science College, Navapur 425 418, India*
[3] *Rani Laxmibai College, Parola 425 111, India*

Nanocomposite ZnO : SnO₂ and pervoskite ZnSnO₃ nanoparticles were synthesized with different volume ratios [40 : 60 (wt %), 50 : 50 (wt %), 60 : 40 (wt %), 70 : 30 (wt %) and 30 : 70 (wt %) respectively] have been deposited by spray pyrolysis technique on glass substrate using an aqueous solution of Zinc chloride (0.1 M) and Stannic chloride (0.1 M) at a substrate temperature $400 \pm 5\,°C$. The structural, surface morphological and optical characterizations of the as-prepared samples were carried out using XRD, SEM, TEM and UV-VIS spectrophotometer, respectively. The XRD result showed nanostructured pervoskite thin films of ZnSnO₃ and composite of ZnO : SnO₂. The volume ratio of zinc chloride and stannic chloride when varied, the particle size was found increasing where as particle shape changed from circular to hexagonal. The X-ray diffraction spectroscopy results indicated that all the samples had the good crystallinity. The ultraviolet-visible absorption spectra showed increased band gap for the samples as compare to the reported values. With the transmission electron microscope, we got some morphology information and evidence to support the UV and XRD analysis results.

**Keywords:** Transparent conducting oxides, Nanocomposite thin films, Pervoskite thin films, Spray pyrolysis, Structural and optical change.

PACS numbers: 68.37.Lp, 78.66.Sq

## 1. INTRODUCTION

Zero and one dimensional nanostructures of binary metal oxides such as SnO₂, ZnO, TiO₂ have attracted great interest owing to their unique properties and potential use in different diverse applications [1-7]. The control of sizes and shapes of nanostructures is crucial as it may affect their electrical and optical properties [8-12]. Use of nanosized building block to fabricate complex structures, an active research is going on [13-16].

ZnO and SnO₂ belong to wide direct band gap semiconductors, and their band gaps are 3.4 and 3.6 eV respectively [17, 18]. Zinc and tin oxides have recently attracted considerable attention and many investigators exploited various synthesis methods to couple and to obtain nanocomposites of ZnO and SnO₂ [19-22]. Transparent conducting oxides such as zinc stannate (ZTO) in the phase space SnO₂-ZnO, whereas ZnSnO₃ is a perovskite-type oxide material. The reported band gap energy of this compound oxide is 3.4-3.6 eV. The band gap values depend on the type of material, single crystal or bulk, method of preparation, size and shape. The data on the synthesis of ZnSnO₃ are ambiguous and contradictory [23], and among the large studies of materials, the details on ternary oxide systems with spinel or perovskite structure have been rarely published [23, 24]. Many methods, including ultrasonic spray pyrolysis [25], thermal evaporation deposition [26-28], chemical vapor deposition [29], hydrothermal synthesis [30-33] and others [34, 35], have been used to produce ZnO, SnO₂ nanoparticles. In this study, ZnO-SnO₂ nanocomposite and nanostructured ZnSnO₃ thin films were synthesized by a simple Spray pyrolysis method. Mixing water soluble Zinc Chloride with Stannic chloride in various proportions was tends to composite of ZnO-SnO₂ and pervoskite of ZnSnO₃ thin films.

## 2. EXPERIMENTAL

Transparent conducting stichiometric nanocrystalline ZnSnO₃ thin films and non stichiometric nanocrystalline composite ZnO-SnO₂ thin films were prepared. All the chemical reagents were analytically pure and used without further purification. Aqueous solution of zinc chloride (ZnCl₄·5H₂O) and stannic chloride (SnCl₄·5H₂O) (Loba chem extra pure) dissolved in double distilled water to a concentration of 0.1 M are used as starting precursors for the preparation of thin films. The stock solution was delivered to nozzle with constant and uniform flow rate of 5 ml/minute using air as a carrier gas. The spray (mist) produced by nozzle was sprayed onto the glass substrates heated at $400 \pm 5\,°C$. Various parameters such as nozzle-to-substrate distance, deposition time, flow rate of solution, deposition temperature and concentration of source solution were optimized to obtain highly textured thin films of good quality. The concentration of Zinc chloride and Stannic chloride precursors are kept fixed and the volume ratio of Zinc chloride and Stannic chloride solution were varied as: 30 : 70, 40 : 60, 50 : 50, 60 : 40 and 70 : 30 (wt %), respectively. The thin film samples with compositions of: 30 : 70, 40 : 60, 50 : 50, 60 : 40 and 70 : 30 were referred as S1, S2, S3, S4 and S5, respectively. The thin films of ZnO : SnO₂ with compositions < 30 : 70 wt % were porous and carried micro cracks and the films at and above 70 : 30 wt % composition were found to be powdery. So the range of compositions for the thin film samples with Zinc chloride and Stannic chloride were taken between 30 : 70 wt % and 70 : 30 wt %. The samples were annealed at 500 °C for 1 hour. Thin films S2, S3, S4 and S5 were found to be the composite of ZnO : SnO₂. Thin films S1 were found to be the pervoskite nanostructured thin films of ZnSnO₃.

---

\* Plalchand_phy_aml@yahoo.co.in

**Table 1** – Spray pyrolysis process parameters for the deposition of $ZnO : SnO_2$ thin films

| Spray parameters | Optimum value/Item |
|---|---|
| Nozzle diameter | 0.1 mm |
| Nozzle-substrate distance | 32 cm |
| Precursor solution concentration | 0.1 M |
| Solvent | Distilled water |
| Solution flow rate | 5 ml/min |
| Carrier gas | Air |
| Gas pressure | 12 Kg/cm$^2$ |
| Substrate temperature Glass | 400 °C ± 50 °C |

## 3. MATERIAL CHARACTERIZATIONS

As prepared films were characterized by X-ray diffractometer (Philips PW 1730) using CuKα ($\lambda = 1.5418$ Å) radiation. The surface morphology and microstructure of the thin films were studied using Transmission electron microscope [CM 200 Philips (200 kV HT)]. The quantitative elemental analysis of the films was estimated by computer controlled energy dispersive X- ray analyzer (model JEOL JSM-6360 Å) attached to the scanning electron microscope. The optical absorption spectra were recorded against wavelengths 300-700 nm using UV-VIS spectrophotometer (SHIMADZU Model UV-2450, Japan) to determine the band gap energy of the samples.
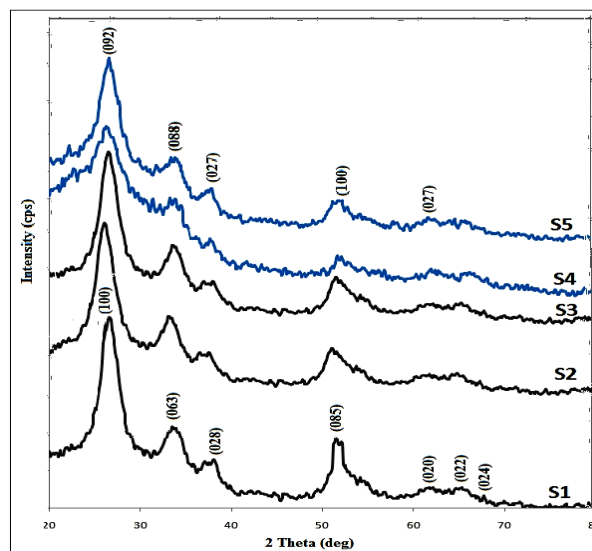
### 3.1 Crystal Structure Using X-ray Diffraction

Fig. 2 shows the X-ray diffractogram of as grown transparent pervoskite sample S1 and composite thin film samples S2, S3, S4 and sample S5. The diffraction peaks from various planes and d-values are matching well with standard ASTM data for ZnO [JCPD#41-1445], $SnO_2$ [JCPD#05-0664] and $ZnSnO_3$ [JCPD#28-1486]. The diffraction spectra for composite thin films of $ZnO : SnO_2$ posses one sharp and three small peaks with crystal planes (092), (088), (027) and (100). It reveals from XRD that the films are polycrystalline in nature. The $ZnSnO_3$ particles had a (100) face-exposed hexahedron structure and the composite $ZnO$-$SnO_2$ particles had a (092) face-exposed octahedron structure. The average grain size for the $ZnO$-$SnO_2$ composite samples and $ZnSnO_3$ samples calculated using Debye-Scherrer formula were 23 nm and 20 nm, respectively.

### 3.2 Elemental Composition

It is clear from the table (1) that the composite thin films are zinc as well as tin rich and oxygen deficient and hence are non stoichiometric in nature. With increase of



**Fig. 1** – XRD pattern of nanocomposite and pervoskite thin films S2, S3, S4, S5 and S1

$ZnCl_4$ in the samples S4 and S5, tin was found deficient and Zinc excess, where as Zinc was deficient and tin excess in the samples S2 and S3. It is clear from the table that the pervoskite thin films S1 was stoichiometric in nature. However, there is a little deviation from stoichiometry of the prepared film.

### 3.3 Surface Morphology

Fig. 2a represents TEM image of nanostructured pervoskite $ZnSnO_3$ thin films sample S1. Fig. 2b-e depicts TEM images of composite nanostructured thin films of samples S2, S3, S4 and S5, respectively. Fig. 2a shows the smaller diameter nanorod of $ZnSnO_3$. It is clear from the images (b-e) that the morphology of synthesized combination of various Zn and Sn thin films are nanoparticles. SEM images in Fig. 2 b-e consist of grains of varying sizes. Along with the smaller spherical grains there are few large grains leading to hexagonal shape. The change in the grains shape was found with respect to the change in the composition of ZnO and $SnO_2$. When volume of $SnCl_4$ is equal to or greater than $ZnCl_4$, the grains were initially seems to be circular in the form of bunch as in Fig. 2b. Image in Fig. 2c shows relatively larger circular shaped grains as compared to Fig. 2b. When $ZnCl_4$ volume is greater than $SnCl_4$, the grains seems to be converting in the hexagonal form as in Fig.2d, and finally the grains were found hexagonal shaped as in Fig. 2e. It seems that the reaction temperature is an important parameter which has influenced the structural morphology of the particles.
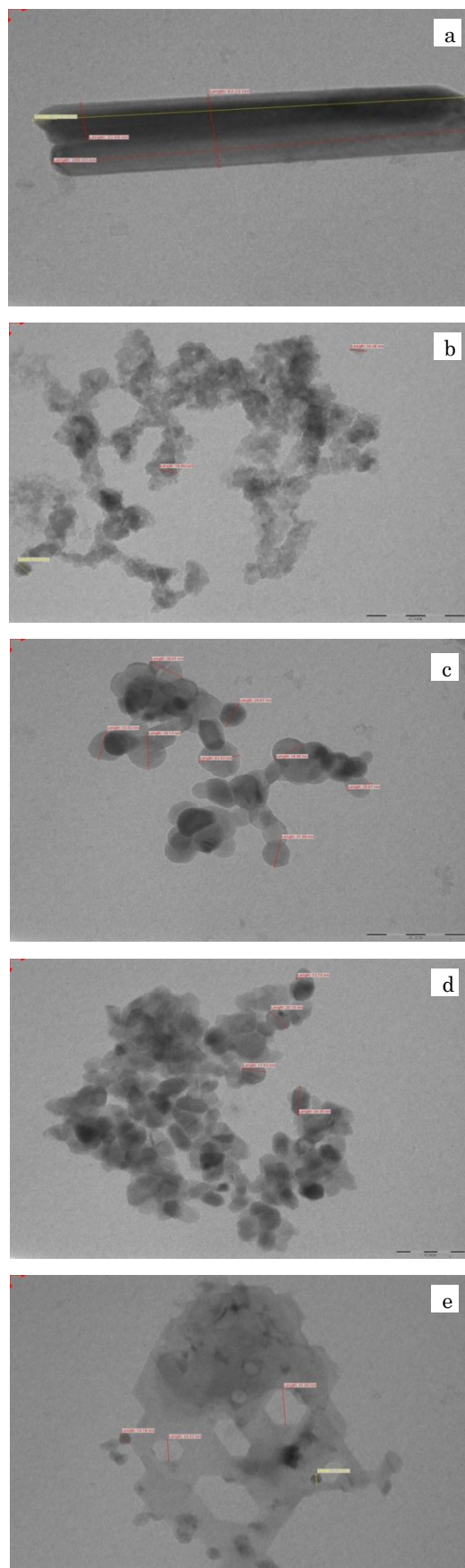
**Table 2** – The composition of composite and pervoskite thin films S2, S3, S4, S5 and S1

| Sample No. | SnCl$_4$.5H$_2$O ml | Addition of ZnCl$_4$·5H$_2$O (ml) | Mass % | | | | | |
|---|---|---|---|---|---|---|---|---|
| | | | SnO$_2$ | Sn | O | O | Zn | ZnO |
| S1 | 70 | 30 | – | 19.68 | 61.76 | | 18.56 | – |
| S2 | 60 | 40 | 61.70 | 31.33 | 30.37 | 17.75 | 20.55 | 38.30 |
| S3 | 50 | 50 | 52.40 | 26.65 | 25.75 | 22.40 | 25.90 | 47.60 |
| S4 | 40 | 60 | 43.10 | 22.53 | 20.57 | 27.25 | 29.65 | 56.90 |
| S5 | 30 | 70 | 31.55 | 14.45 | 17.10 | 34.60 | 33.85 | 68.45 |

**Fig. 2** – TEM images of pervoskite and nanocomposite thin film for samples: (a) S1, (b) S2, (c) S3, (d) S4 and (e) S5.
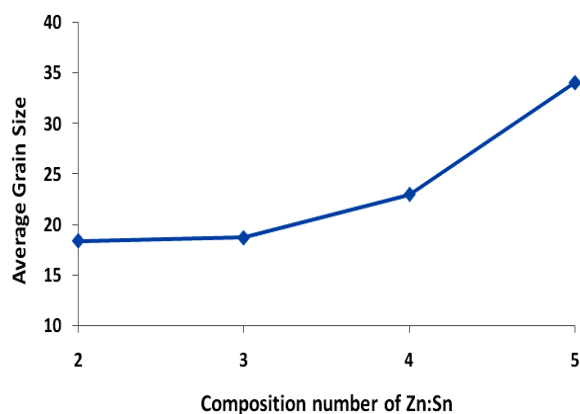


**Fig. 3** – Relationship between compositions of Zn : Sn and average grain size

Formation of one-dimensional nanostructure requires anisotropic growth of material, i.e. the crystal should grow along a certain orientation faster than the other directions. The driving force for the synthesis of nanorods is the decrease in Gibbs free energy because of low super saturation. At elevated temperature $400 \pm 5\,°C$ suitable conditions are met, resulting in the synthesis of pervoskite $ZnSnO_3$ nanorods. At an elevated temperature due to high super saturation there is no reduction in Gibbs free energy, which results in homogeneous nucleation leading to isotropic growth of zinc and tin oxide, and we get isotropically grown particles instead of rods [36]. The change in the mean grain size as a function of composition of Zn : Sn is presented in Fig. 3. The results indicate that the average grain sizes of samples increase steeply from 18.41 nm to 34.07 nm. Table 2 shows average grain size of as-prepared samples for various volume ratio of Zn : Sn. The composition 1 corresponds to $ZnSnO_3$ nanorod and it has the dimension as $31.11 \times 255$ nm.

**Table 2** – Average grain size of composite and pervoskite thin films  S2, S3, S4, S5 and S1.

| Composition No. | Compositions of Zn:Sn | Average grain size(nm) |
|---|---|---|
| 1 | 30:70 | 31.11 X  255 |
| 2 | 40:60 | 18.41 |
| 3 | 50:50 | 18.73 |
| 4 | 60:40 | 23.02 |
| 5 | 70:30 | 34.07 |

### 3.4  Absorbance Spectra

Fig. 4 shows the absorbance spectra of nanostructured thin films for various Sn and Zn compositions and pervoskite $ZnSnO_3$ thin films synthesized on glass substrates. The absorption spectra of the samples (S1-S5) were recorded in the wavelength range 200-700 nm using UV-VIS spectrophotometer. It is clear from the figure that the absorption edge shifts towards the lower wavelength side with increase in SnCl4, and there is blue shift in absorption edge. The sprayed films were transparent in the visible with a sharp UV cutoff at 370 nm. The absorbance of pervoskite $ZnSnO_3$ thin film sample (S1) is larger than the absorbance of composites samples (S2, S3, S4 and S5). The band gap energy calcu-

lated form absorbance spectra are 4.13, 4.06, 4.00, 3.95 and 3.91 eV of samples S1, S2, S3, S4 and S5 respectively. Reported band gap of $ZnSnO_3$ is 3.6 eV. The band gap of $ZnSnO_3$ was observed to be enhanced (4.13 eV) as compared to the reported band gap (3.6 eV). It may be due to nanocrystalline nature of the film.
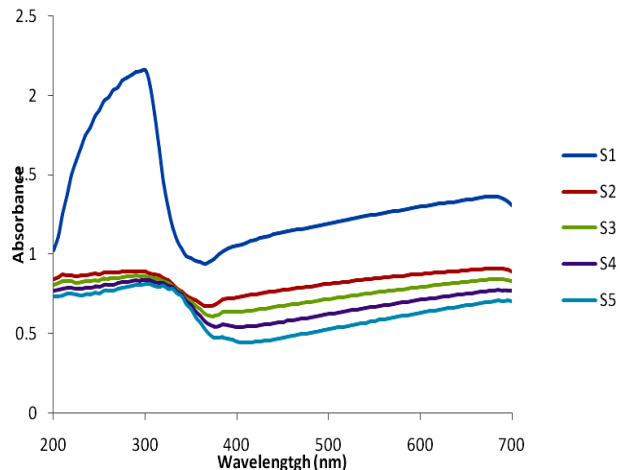


**Fig. 4** – Absorbance spectra of nanocomposite and pervoskite thin films S2, S3, S4, S5 and S1

## 4.  CONCLUSIONS

Nanostructured composite thin films of $ZnO : SnO_2$ and pervoskite $ZnSnO_3$ thin films were successfully prepared by simple spray pyrolysis technique.

Grains of Nanostructured composite thin films of $ZnO : SnO_2$ and pervoskite $ZnSnO_3$ thin films are found to be polycrystalline in nature.

The structural and microstructucal properties of samples showed the nanostructures in S1, S2, S3, S4 and S5 samples.

Surface morphological study of Nanocomposite thin films of $ZnO : SnO_2$, showed that the average grain size ranges from 18 nm to 34 nm.

The band gap energy of S1, S2, S3, S4 and S5 samples was observed to be 4.13, 4.06, 4.00, 3.91 and 3.91 eV. The band gap of $ZnSnO_3$ was observed to be enhanced (4.13 eV) as compared to the reported band gap (3.6 eV). It may be due to nanocrystalline nature of the film.

## REFERENCES

1.  S. Baruah, R.F. Rafique, J. Dutta, *J. Nano* **3**, 399 (2008)
2.  A. Fujishima, T.N. Rao, D.A. Tryk, *J. Photochem. Photobiol. C* **1**, 1 (2000).
3.  A. Aguedach, S. Brosillon, J. Morvan, E.K. Lhadi, *Appl. Catal. B* **57**, 55 (2005).
4.  J.B. Baxter, E.S. Aydil, *Appl. Phys. Lett.* **86**, 053114 (2005).
5.  T. Bora, *Studies on zinc oxide nanorod dye-sensitized solar cell Master Thesis AIT* (2009).
6.  S. Chappel, A. Zaban, *Sol. Energ. Mater. Sol. C.* **71**, 141 (2002).
7.  T. Bora, H.H. Kyaw, M. Poyai, J. Dutta, *The 3rd Thailand Nanotechnology Conf. Asian Institute of Technology* (Bangkok: 21-22 December: 2009).
8.  K. Arshak, I. Gaidan, *Mater. Sci. Eng. B* **118**, 44 (2005).
9.  E. Comini, G. Faglia, G. Sberveglieri, Z. Pan, Z.L. Wang, *Appl. Phys. Lett.* **81**, 1869 (2009).
10. M.K. Hossain, S.C. Ghosh, Y. Boontongkong, C. Thanachayanont, J. Dutta, *J. Metastable Nanocryst. Mater.* **23**, 27 (2005).
11. G. Lu, K.L. Huebner, L.E. Ocola, M. Gajdardziska-Josifovska, J. Chen, *J. Nanomater.* **2006**, 60828 (2006).
12. K. Nomura, H. Ohta, K. Ueda, T. Kamiya, M. Hirano, H. Hosono, *Microelectron. Eng.* **72**, 294 (2004).
13. T. Lana-Villarreal, G. Boschloo and A. Hagfeldt, *J. Phys. Chem. C* **111**, 5549 (2007).
14. M. Miyauchi, Z. Liu, Z.G. Zhao, S. Anandan, K. Hara, *Chem. Commun.* 46, 1529 (2010).
15. B. Tan, E. Toman, Y. Li, Y. Wu, *J. Am. Chem. Soc.* **129**, 4162 (2007).
16. I. Stambolova, K. Konstantinov, D. Kovacheva, P. Peshev, T. Donchev, *J. Solid State Chem.* **128**, 305 (1997).
17. A. Alkaya, R. Kaplan, H. Canbolat, S.S. Hegedus, *Renew. Energ.* **34**, 1595 (2009).
18. X. Song, Z. Wang, Y. Liu, C. Wang, L. Li, *Nanotechnology* **20**, 075501 (2009).
19. J.H. Yu, G.M. Choi, *Sensor. Actuat. B* **52**, 251 (1998).
20. Q. Kuang, Z-Y. Jiang, Z-X. Xie, S-C. Lin, Z-W. Lin, S.Y. Xie, R-B. Huang, L-S. Zheng, *J. Am. Chem. Soc.* **127**, 11777 (2005).
21. M. Zhang, G. Sheng, J. Fu, T. An, Z. Wang, X. Hu, *Mater. Lett.* **59**, 3641 (2005).
22. C. Liangyuan, B. Shouli, Z. Guojan, L. Dianquing, C. Aifn, C.C. Liu, *Sensor. Actuat. B* **134**, 360 (2008).
23. J. Xu, X. Jia, X. Lou, J. Shen, *Solid-State Electron.* **50**, 504 (2006).
24. H. Zhu, D. Yang, G. Yu, H. Zhang, D. Jin, K. Yao, *J. Phys. Chem. B* **110**, 7631 (2006).
25. U. Alver, T. Kilinc, E. Bacaksiz, T. Kuecuekoemeroglu, S. Nezir, I.H. Mutlu, F. Aslan, *Thin Solid Films* **515**, 3448 (2007).
26. H.B. Cheng, J.P. Cheng, Y.J. Zhang, Q.M. Wang, *J. Cryst. Growth* **299**, 34 (2007).
27. P. Klason, K. Magnusson, O. Nur, Q.X. Zhao, Q.U. Wahab, M. Willander, *Phys. Scripta* **126**, 53 (2006).
28. L. Khomenkova, P. Fernandez, *Cryst. Growth Des.* **7**, 836 (2007).
29. F. Paraguay, W. Estrada, L.D.R. Acosta, N.E. Andrade, M. Miki-Yoshida, *Thin Solid Films* **350**, 192 (1999).
30. O. Lupan, L. Chow, G.Y. Chai, B. Roldan, A. Naitabdi, A. Schulte, H. Heinrich, *Mater. Sci. Eng. B* **145**, 57 (2007).
31. Z.Y. Huang, C.F. Chai, B.Q. Cao, *Cryst. Growth Des.* **7**, 1686 (2007).
32. R.B. Kale, S.Y. Lu, *J. Phys.: Condens. Matter* **19**, 096209 (2007).
33. Y.J. Kim, C.H. Lee, Y.J. Hong, G.C. Yi, S.S. Kim, H. Cheong, *Appl. Phys. Lett.* 89, 63128 (2006).
34. C.L. Kuo, T.J. Kuo, M.H. Huang, *J. Phys. Chem. B* **109**, 20115 (2005).
35. J.M. Du, Z.M. Liu, Y. Huang, Y.N. Gao, B.X. Han, W.J. Li, G.Y. Yang, *J. Cryst. Growth* **280**, 126 (2005).
36. Ravi Chand Singh, Onkar Singh, Manmeet Pal Singh, Paramdeep Singh Chandi, *Sensor. Actuat. B* **135**, 352 (2008).